

Paper No. 12

A STUDY OF THE TECHNIQUES OF DYNAMIC
ANALYSIS OF HELICOPTER TYPE STRUCTURES

G.M. Venn
D.J. Boon

Westland Helicopters Limited
Yeovil Somerset
England

September 8 - 11, 1981

Garmisch-Partenkirchen
Federal Republic of Germany

Deutsche Gesellschaft für Luft und Raumfahrt e.V.
Goethestr. 10, D-5000 Köln 51, F.R.G.

1. INTRODUCTION

Westland Helicopters Limited (WHL) has been using finite-element techniques for many years for the analysis of the dynamic or vibrational characteristics of helicopters. The finite element system used for all this work is the commercially available MSC/NASTRAN program. Natural frequencies and mode shapes of vibration are calculated using the program and these are used with predicted rotor-head forces to calculate the vibration response of the airframe.

During the analyses of the helicopters, comparisons were made with experimental shake tests on the aircraft. The comparisons were not always satisfactory and many problems were highlighted which could not be resolved owing to the large scale of the analyses and the difficulties of access to the airframes for further experimental work.

A programme of work was undertaken to improve the confidence of the Company in the use of finite-element methods and to investigate the difficulties of making experimental comparisons. Due to cost and time-scale limitations an analysis of a complete helicopter could not be made, so a small test piece was designed and built.

This test piece was constructed from aircraft materials to aircraft standards and tolerances. Various modelling problems were incorporated into the design of the test piece. These are:

- (a) Riveted panel-stringer constructions
- (b) Deep fabricated beams
- (c) Discontinuous load paths
- (d) Bolted joints
- (e) Honeycomb panels
- (f) Simulated gearbox
- (g) Simulated engine mounts
- (h) Simulated engine mass

It was designed such that increasing the build state added one or two extra modelling problems. To provide a useful correlation exercise three separate studies were performed on the test piece.

- (i) Vibration testing to provide natural frequencies and mode shapes.
- (ii) A dynamic analysis using the MSC/NASTRAN finite-element program to provide natural frequencies and mode shapes.
- (iii) An alternative and independent analysis using the PAFEC finite element system.

The vibration testing was carried out at Imperial College using single-point excitation techniques. Some of this work is reported in paper no. 13 of this Forum by Dr. D.J. Ewins, and a few of the more relevant points will be mentioned here.

The NASTRAN analysis was made by WHL and the independent PAFEC analysis was made by Structural Dynamics Limited.

2. DESCRIPTION OF TEST PIECE

An exploded view of the test piece is shown in figure 1. It comprises an upright fabricated beam attached to a base. The base is fixed into earth by several mounts. On the top of the upright beam, simulated engine and simulated engine mounts are fitted. Finally a honeycomb panel can be fitted to the side of the upright beam.

The test piece was fixed into earth rather than being tested free-free to enable static stiffness measurements to be made for comparison with some theoretical predictions. This work is not presented here.

The components of the test piece are described below.

Base

The base is a lattice arrangement of deep fabricated beams with a bottom aluminium skin. The beams in the x-direction are continuous deep beams i.e. two thick L-section stringers with a plate riveted in between. The beams in the y-direction are not continuous across the structure and consist of a number of stiffeners and plates riveted together. Therefore depending on the direction of bending the analysis should be able to differentiate between the continuous and discontinuous beams.

Beam

The beam is a fabricated structure. It is a box section consisting of six vertical stringers with a skin on three sides, the other side being open for the sandwich panel to be added when needed. There are four stiffening diaphragms inside the beam, each having a different configuration of 'lightening' holes. The beam is attached to the base through a number of bolts which constitute a transport-type joint.

Simulated Engine Mounts

These represent an engine mounting system on a helicopter. A fabricated mounting bracket is attached to the beam through a row of bolts. The simulated engine mass is then attached to the bracket by two 'V' mounting arms and one vertical connection. The 'V' arms are allowed to pivot about the three points of the 'V'. The vertical connection allows rotation about the vertical direction. In a real case these joints would be ball joints causing a statically determinant system i.e. no moments would be transmitted to the engine. However, due to the lack of available components simple pivots were chosen to simulate the engine mounts.

Simulated Engine Mass

The simulated engine mass is a braced 'L' section made of 3/16" thick steel plate. The mass of this simulated engine was approximately half of the total mass of the complete test piece.

Honeycomb Panel

The honeycomb panel is a typical helicopter aluminium honeycomb structure. It has two 0.3 mm thick skins with a 12 mm thick CIBA Aeroweb 5052 aluminium core. This panel could be bolted to the open face of the beam along all its edges.

Base Mounts

The base of the structure is mounted to the laboratory test platform by eight base mounts. These are of a braced steel construction and are fixed to the ends of the lattice of deep beams on the base.

Four build cases were studied, each build case adding one or two extra modelling problems. A description of the build cases is given below starting with the simplest configuration.

Build Case A

Build A consists of the beam, base and base mounts. This is the least complicated build state which contains continuous and discontinuous fabricated beams and bolted joints. This build is intended to simulate a typical airframe structure without any large concentrated masses. It is the basic build for all the other cases.

Build Case B

This build state takes the basic build state, with the simulated engine mass mounted directly on the top of the beam through four bolts and spacers. This build shows the effect of a large mass mounted directly onto a relatively flexible structure and is analogous to a gearbox mounted on an aircraft fuselage.

Build Case C

This build state simulates the effect of an engine mounting mechanism on a helicopter structure. It consists of Build Case A with the simulated engine mounts and mass bolted to the top of the beam.

Build Case D

This is the most complex build state with all the components being used including the honeycomb panel. The addition of the honeycomb panel increases the damping and stiffness of the structure, also making it more symmetric in bending. This build case is probably the most representative of current helicopter structures.

3. EXPERIMENTAL TESTS

The test piece was attached to a massive floating bed by the base mounts. Accelerometers were attached to the structure at points corresponding to GRID (element connection points) points of the NASTRAN model. Excitation was applied at a single point and the direct and cross inertances measured at the transducer positions (inertance = harmonic acceleration response divided by excitation force). From the inertances the mobilities, receptances and the modal properties were derived.

All the build cases were tested in the frequency range of 0 Hz to 300 Hz and by analysing the inertance measurements the following results were obtained for each build state.

- (a) The natural frequencies between 0 Hz and 300 Hz.
- (b) The associated damping for each mode of vibration.
- (c) The values of the eigenvectors for each mode normalised to unit generalised mass.
- (d) Mode shape plots.

These results (with the exception of the damping) could be compared directly with the finite-element calculations.

During the experiments, several problems became apparent. Slight non-linearities were observed such that increasing the exciting force caused the mobilities (or inertances) to alter and the resonant frequencies

to change slightly. Up to two percent reductions in frequency were obtained when the force levels were increased from approximately 0.5N to 10N. These changes in mobilities and frequencies are indicative of dry friction and cubic stiffness effects in the structure. To reduce the effects of the non-linearities very low force levels were used.

Some of the measuring positions showed marked sensitivities to the exact location of the transducer, especially in the mobility results which affected the value of the eigenvectors at these points. At one point in some of the modes, variations of up to 20% in displacement were obtained by moving the measuring accelerometer only one inch on a reasonably stiff bracket. Two reasons were attributed for causing this effect, the change in local stiffness and the presence of nearby nodal lines at some frequencies.

The measurements showed fair repeatability. After the structure had returned from another location following some static measurements, the frequencies and inertances were checked at several points. The largest change found in the natural frequencies was 1.5% on a torsion mode with corresponding changes of up to 30% in some of the eigenvector displacements.

The above limitations in the experimental work must be remembered when making comparisons with the predicted results from the finite element analyses.

4. FINITE ELEMENT ANALYSES

4.1. Analysis using MSC/NASTRAN

A NASTRAN finite-element model was set up for the various configurations. It had six sections which could be interchanged and connected depending on the build state. The modelling was done directly from drawings giving virtually a one-to-one model of NASTRAN and physical elements.

The model of the most complicated build state, Build D, is shown in figure 2. The base is modelled as a lattice of bars and plate elements. The deep cross beams were represented by bar elements for the flanges and plate elements for the webs. The base mounts were modelled by plate elements and attached directly onto the cross beams of the base and fixed into earth by spring elements representing the mounting bolts.

The beam was modelled as a box section with six vertical stringers with the three sides being covered by plate elements representing the skins. The various stiffening bay dividers were modelled by plates with rod elements for the stiffening edges and lips. The beam was attached to the base at ten points by rigid elements.

The engine mounting structure was modelled by plate elements and the two supporting vee arms were modelled by bar elements with the rotational degrees of freedom at the ends released to represent the pin joints. The other vertical connection on the mass was allowed to rotate about the vertical direction.

The engine mass was modelled by plate elements and attached to the engine mounts by pin joints at the mounting arms.

The honeycomb panel was modelled by plate elements. It was assumed that all the transverse shear was taken by the aluminium honeycomb and that the membrane and bending actions were carried by the skins.

The model for the most complicated build state, Build D had 1186 degrees of freedom and 504 elements. The total mass was 74.3 kg of which approximately half was accounted for by the simulated engine mass.

The modulus of elasticity of the aluminium alloy was originally taken from material property tables as 71.7 kN/mm². However, tensile tests performed on specimens of the aluminium from which the test piece was made gave a spread of values from 67.4 to 69.8 kN/mm². An average of 68.5 kN/mm² was used in the model.

Each build state was analysed to find the natural frequencies and mode shapes. The large number of degrees of freedom in the models were not required in the dynamic analysis because the frequency range was restricted to 300 Hz. Analysing the complete sets of degrees of freedom would extract frequencies far higher than 300 Hz so a reduction was made in the number of freedoms using the Generalised Dynamic Reduction Technique available in Version 48 of MSC/NASTRAN. The problem was formulated by a set of generalised degrees of freedom which are modal coordinates. The program determines approximately how many modes lie in the frequency range and sets the number of generalised freedoms to 1.5 times this number for use in the extraction of the natural frequencies and mode shapes.

Large reductions in the number of degrees of freedom were made, from approximately 1000 in the complete models to 30 in the reduced models.

The final mode shapes and frequencies were extracted using the Given's Method. Comparisons of the calculated and measured frequencies are shown in figure 3 using visual comparisons made from plots of the mode shapes.

In all the Builds, the NASTRAN models predicted more modes than were found in the experiments. These extra modes were very localised or panel modes which would not be detected in the experiments unless a transducer was positioned on the panel of interest. However, it is unlikely that the panel-mode frequencies calculated by the program will be accurate because the reduced models are not sufficiently fine to represent these local areas accurately enough. Therefore no attempt was made to locate these panel modes in the experimental work.

The important modes are those which involve larger or structural deflections such as lateral bending or torsion of the upright beam. In all of the build cases the major structural modes found during the experiments were also found in the NASTRAN models.

For Build A, the simplest build case, good agreement was found for the frequencies with the largest difference being 7%. This result was achieved after two or three analyses when it was discovered that the vertical bending stiffnesses of the deep beams in the base were 6% over stiff because the lines of GRID or element connection points lay at the extreme top and bottom of the deep beams so that the neutral axes of the flanges were too widely spaced.

Another problem with the position of neutral axes occurred in the vertical stringers on the upright beam. The neutral axes were incorrectly assumed to lay in the line of the skins making the upright beam 8% over stiff. To correct this, neutral axis offsets were included in the bar elements.

The mounts, which fixed the structure into 'earth' were modelled explicitly. Originally the cross beams on the base were fixed directly into earth at the ends, but it was found that the mounts were significantly flexible, dropping the frequency of the fundamental bending modes by 2 Hz in approximately 70 Hz when they were included in the model.

The final frequency comparisons for this build state were good, with the largest error occurring on the fourth structural mode of approximately 7%. Apart from this mode, the other comparisons show that the finite-element model is over stiff which is to be expected when using the displacement approach in the finite-element system. The anomaly in the trend in the last mode is thought to be due to the fall off in accuracy of the extraction technique at the end of the frequency range.

The results for Build A show the good ability of NASTRAN to model a riveted structure. The frequency comparisons were close enough (less than 10% to be of use in forced-response calculations.

Build B took the basic Build A with the simulated engine mass bolted directly onto the top of the upright beam.

The frequency comparisons (figure 3) show poor agreement for two of the modes, both of which have significant motion of the engine mass. The engine mass had been modelled as rigid with rigid connections to the top of the upright beam. It was found in subsequent analyses of other build states that the mass possessed significant flexibility and this is what caused the two large errors. However, reasonable comparisons were obtained for the other flexural-type modes.

The results from this build show that care must be taken before assuming areas of structures to be rigid and the interface between the 'stiff' and flexible regions of the structure must be modelled carefully.

Build C took the basic build with the engine mounts and engine mass bolted onto the top of the upright beam. The engine mass and mounts were modelled explicitly in this analysis. The original assumption of rigidity for the mass was really based upon our experience with aircraft structures where the frequency range of interest is below 40 Hz and in this range the mass behaved as a rigid body. The first flexural mode of the mass occurred at about 80 Hz and so flexure of this component is relevant because of the small scale of the model and the higher frequency range.

The frequency comparison (figure 3) for this build shows fair comparison. All of the modes except one had errors of 9% or less. The largest error of about 13% occurred on a vertical bounce mode. Unfortunately no vertical transducer was used during the experiments in this build and the exciter was horizontal so the comparison for this mode was based upon transducers lying in the other directions which had much smaller deflections.

All the modes above 90 Hz have some flexural motion of the engine mass. This area had few transducers in the experiments and in hindsight this was a serious deficiency in this part of the experimental work.

The results show that the engine mount structure, including the flexible arms and pin joints, has been modelled reasonably well although the error margin has again increased.

Build D is the most complicated build state, with the sandwich panel being added onto Build C. The frequency comparisons are good except for the fundamental bending in the x-direction. The large error is thought to be due to incorrect modelling of the in-plane shear stiffness of the sandwich panel.

Vertical transducers were used in this build, and the vertical bounce mode had a 10.9% error, slightly smaller than in Build C.

All of the higher frequency modes involved significant deformation of the engine mass but several extra transducers were used on the mass in the experiments enabling the mode shape comparisons to be made easily.

The mode shape comparisons were made by visual inspection of plots of the deformed structure, such as those shown in figures 4 and 5 which are plots of the torsion of the top mass and the vertical bounce modes in Build D. Visual inspection of plots enables a qualitative comparison to be made.

Quantitative comparisons can be made using the eigenvectors. By plotting the NASTRAN eigenvector against the experimental eigenvector for each point in turn a straight line graph should be obtained with a slope of one (since each eigenvector was normalised to unit generalised mass). Plots of this type for the two modes shown in figures 4 and 5 are presented in figures 6 and 7.

These graphs show the difficulties of comparing point displacements in the structure. As stated in Section 3 the measurements can vary significantly when the transducer position is changed by a small distance. The NASTRAN program gives deflections at points whose positions are defined by the connection of elements. Choosing a corresponding point on the structure is difficult. This may account for some of the scatter in the points.

The facts, also given in Section 3, about the repeatability and non-linearity of the measured eigenvectors should also be remembered when making this type of quantitative comparison.

The excitation point is shown on the figures. If this point is close to the origin of the graph, it has a small displacement compared with the other points in the structures. Therefore it may not be the best point to apply excitation for the particular mode because it may not be 'well coupled' to that mode. It is also used to scale the rest of the eigenvector. This sort of graph can therefore help in choosing effective excitation points, and these points may be different points for the various modes.

These two graphs are not the best that were obtained. They were picked to show the difficulties in making comparisons. However the modes show reasonable agreement and the figures show how a quantitative comparison can be made which may be useful for complicated mode shapes.

During this study, a comparison was made of the two reduction techniques available in MSC/NASTRAN. These are the Generalised Dynamic Reduction (G.D.R.) method which has been available for about two years, and the more traditional Guyan Reduction technique.

The major difference between the two techniques is that Guyan Reduction uses a static condensation approach with the reduced degrees of freedom being chosen by the user. Generalised Dynamic Reduction

uses a set of modal coordinates which are automatically produced by the program. Larger reductions are available with G.D.R. because the reduced number of degrees of freedom is 1.5 times the number of modes in the frequency range of interest. To obtain an adequate definition of the structure using Guyan Reduction requires many more degrees of freedom than this.

Three test cases were analysed using Build C which is the basic structure with the engine mass mounted onto the top of the upright beam via the engine mounts. The engine mass was modelled by a single concentrated mass and attached to the top of the beam by rigid elements with pin joints corresponding to the engine links. As shown earlier, the mass is not rigid and should be modelled by flexural elements. However, the point mass model was chosen because this is a technique used on aircraft to model high-mass regions.

The engine mass had inertias included in the unreduced model. The three test cases were:

- (i) RUN 1 - full G.D.R. reduction from 1440 degrees of freedom to 32.
- (ii) RUN 2 - Guyan reduction to 69 degrees of freedom with three translational freedoms only on each analysis point (including engine mass).
- (iii) RUN 3 - As RUN 2 with all six degrees of freedom on the engine mass.

The Guyan degrees of freedom were chosen to give a good distribution throughout the structure.

The frequency results are shown in figure 8. Differences in frequency were obtained for all three runs. The largest difference of around 12% occurred in RUN 2 with the three degrees of freedom only on the mass. The two bad modes both involved rotational movements of the mass. Placing all the six degrees of freedom at the mass in the reduced set, RUN 3, improved the correlation of one of these modes. However a difference of about 10% was still apparent in one mode.

This mode is a second torsion mode of the upright beam and the error is probably due to the inadequate representation of the torsional stiffnesses and inertias in the reduced set of freedoms.

This set of analyses showed that significant differences in frequency can be obtained when using the different analysis methods further complicating the comparisons with the experimental work.

4.2. Analysis using the PAFEC System

This analysis was made, independently, by Structural Dynamics Limited using the PAFEC finite-element system.

Considering only Build D, the most complicated build, the PAFEC model was created in a similar manner to the NASTRAN model. It had approximately twice the degrees of freedom of the corresponding NASTRAN model because of the use of elements with midside nodes throughout the model.

The Guyan reduction technique was used, reducing the freedoms to 78. Frequencies and mode shapes were extracted. The frequencies are shown in figure 9.

The errors are similar to those obtained in the NASTRAN analysis, figure 3. The largest error occurs for the same mode as the NASTRAN analysis showing that, again, an error has been made in the modelling of the sandwich panel. The other large errors are greater than in the NASTRAN analysis and may be due to the reduction technique used.

5. CONCLUDING REMARKS

The object of analysing structures using finite elements is to predict the dynamic behaviour of the structure. For helicopters, this means investigating how the structure behaves when subjected to rotor head forcing. That is, it is essentially a forced response problem.

The natural frequencies and normal modes can be used to calculate the forced response. To be of any use, the calculated frequencies should be within 10% of the actual or measured values, and preferably less than this.

This study has shown how difficult it is to achieve this accuracy. Problems were encountered in both the experiments and finite element work which made the comparisons difficult.

During the experimental work, non linearities were observed in the test piece which lead to variations of up to 2% in frequency when the forcing levels were increased. Variations were also observed in the repeatability when the structure was re-tested of 1.5% on frequency and up to 30% in the displacements.

Another major problem was the variation in displacements (up to 20%) obtained when slightly moving the position of the transducers. This makes comparing the displacements with the finite element results very difficult, especially for the smaller displacements.

The NASTRAN results for the simplest build (Build A) had less than 10% errors in frequency for all the modes. This was only obtained after problems with the neutral axis positions on the beams had been corrected.

The structural modes in Build B were also better than 10% in the frequency comparisons. The two large errors in this build were due to the assumption of the engine mass being rigid. This may not be as large a problem for helicopters because of the much lower frequency range of interest, however it shows that care must be taken when assuming rigidity for large components such as frames.

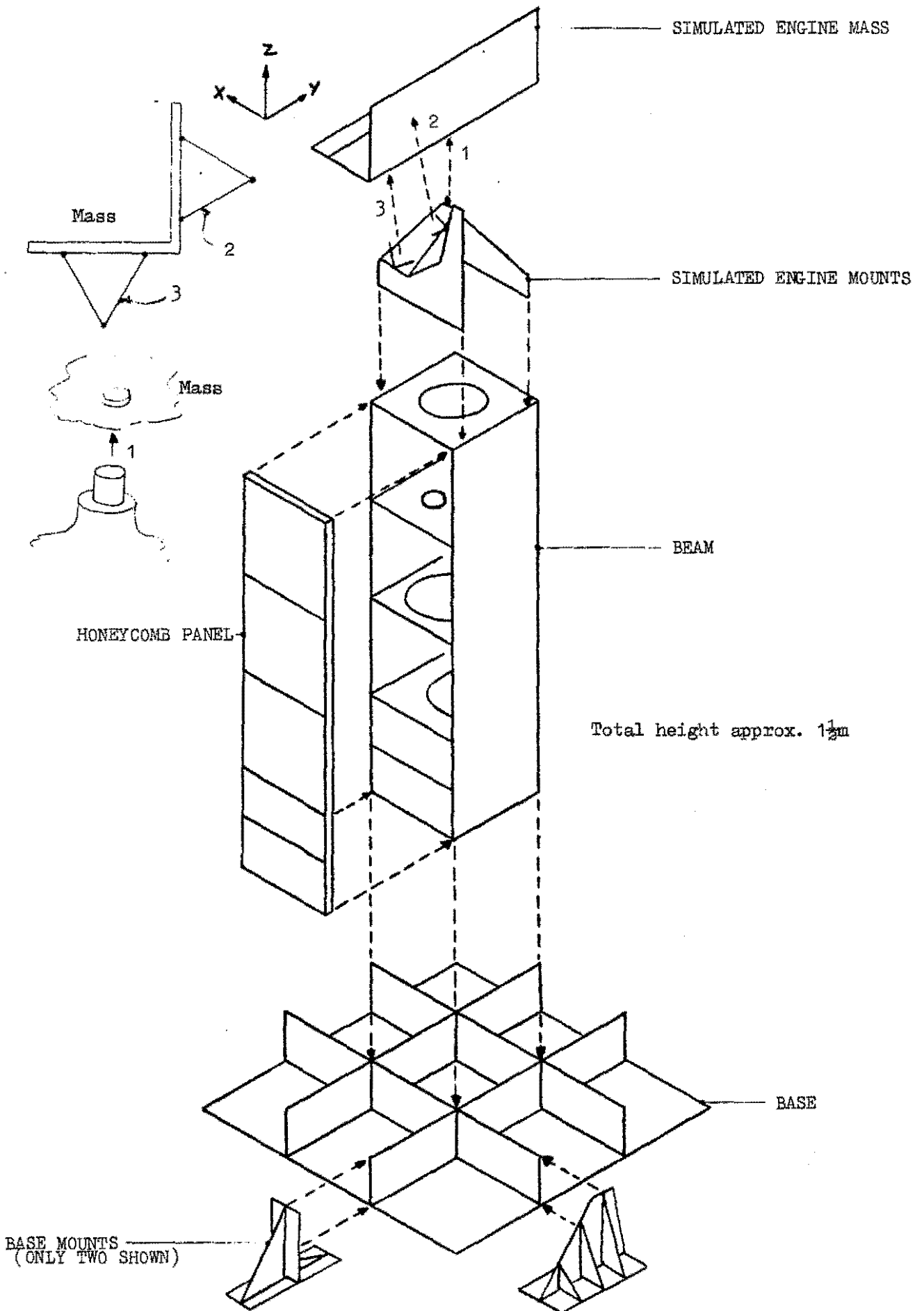
The NASTRAN program handles pin joints well as the results for Build C show. Only one mode in this build had more than the 10% error in frequency. This was a vertical bounce mode, and may be due to the lack of a transducer acting in the vertical direction.

The error margins increased slightly in Build D. Two of the frequency errors were about 11% and the largest was 18% which is attributed to incorrect modelling of the properties of the honeycomb panel. This is confirmed by the PAFEC results for this build which showed great similarity to the NASTRAN results.

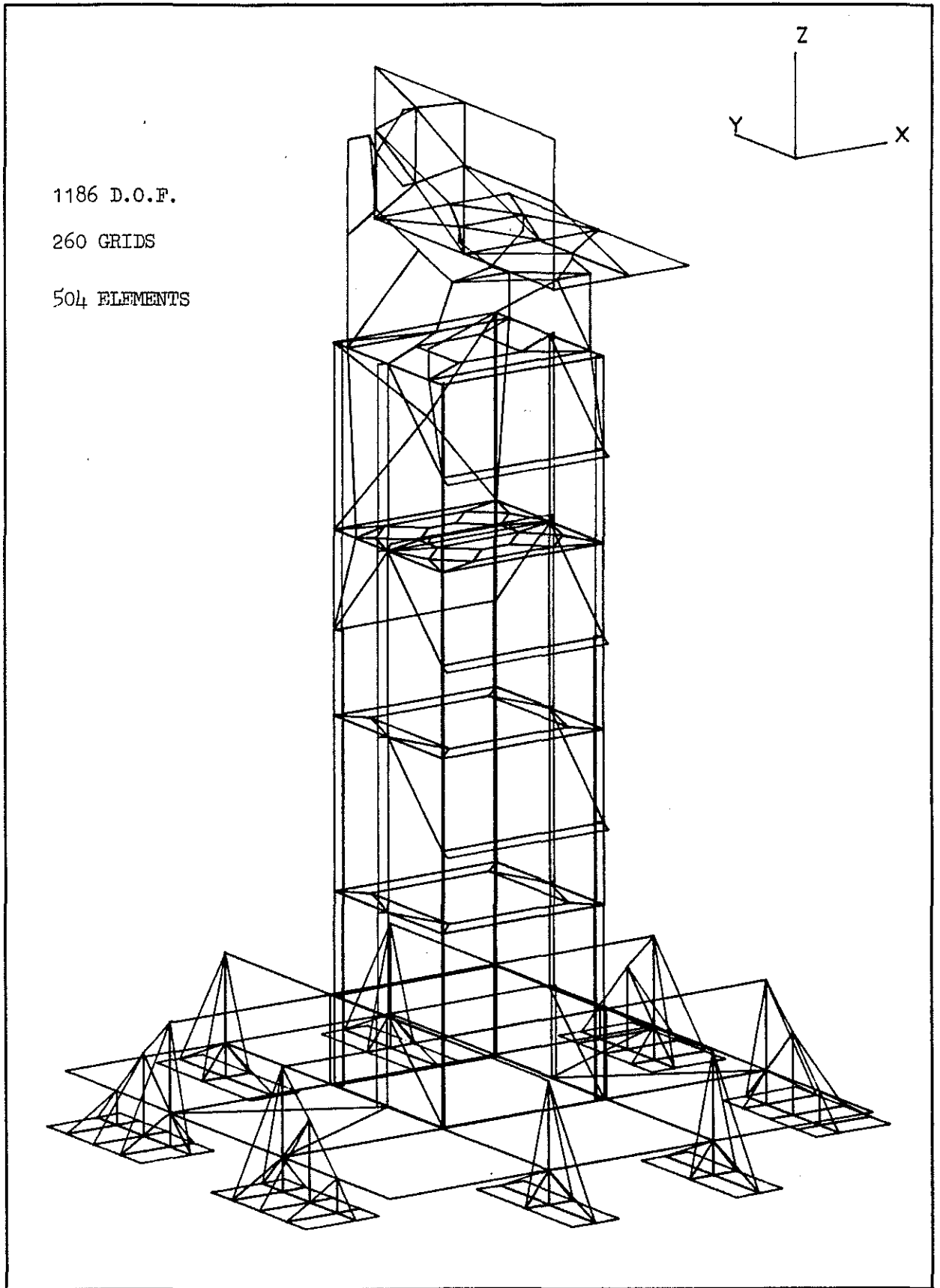
Modelling techniques were not the only problems encountered in the finite element work. The reduction technique could also affect the results. Differences of 10% in frequency were obtained when using Generalised Dynamic Reduction and Guyan Reduction.

In general, errors of less than 10% in frequency can be obtained, but only after refining the finite element models, and re-testing any suspicious modes. It is important to remember that difficulties will be encountered on both the experimental and theoretical sides of the work.

TEST PIECE COMPONENTS



NASTRAN MODEL OF BUILD D



MODAL FREQUENCY COMPARISON

BUILD A

Description	Test Results (Hz)	NASTRAN Frequency (Hz)	% Error
1st Bending - X Direction	65.33	68.66	5.1
1st Bending - Y Direction	123.066	129.20	4.98
Base Plate Panel Modes		(148.3 (149.8 (152.0 (153.4	
Vertical Panel Mode	142.7		
Side Panel Mode		196.3	
Torsion	201.5	212.07	5.24
Torsion + Panel Mode		212.08	
Vertical Panel Mode		220.28	
Vertical Panel Mode	255.2		
2nd Bending + Torsion	286.7	266.43	-7.06

BUILD B

Description	Test Results (Hz)	NASTRAN Frequency (Hz)	% Error
1st Bending - X Direction	19.54	20.82	6.55
2nd Bending - Y Direction	39.30	41.85	6.49
Torsion	68.46	74.27	8.38
Top Mass Vertical	79.16	104.8	32.3
Top plate X Direction + Torsion	99.17	108.05	8.95
Top Panel Y, Mass Y in anti-phase + torsion	149.6	120.05	-19.4
Base panel modes		(148.3 (149.8 (152.0 (153.4	
Second torsion + Mass Y	213.5	228.0	6.8
Top plate vertical		286.7	

BUILD C

Description	Test Results (Hz)	NASTRAN Frequency (Hz)	% Error
1st Bending - X Direction	20.54	22.4	9.05
1st Bending - Y Direction	32.19	34.85	8.26
Torsion about Z	61.51	66.99	8.91
Top Lozenge	86.82	89.36	2.92
Vertical bounce + y bending	143.5	162.5	13.24
Base plate panel modes		(148.4 (149.8 (152.1 (153.4	
Mass Panel mode		168.0	
Panel mode?		183.65	
2nd Bending about Y + torsion	216.9	201.65	-7.03
3rd Bending in X direction + torsion	231.6	225.2	-2.76
3rd Bending in Y direction + torsion		240.2	
Mounts Panel Mode		263.15	
Mounts Panel Mode		279.15	
Top Plate panel mode		297.8	

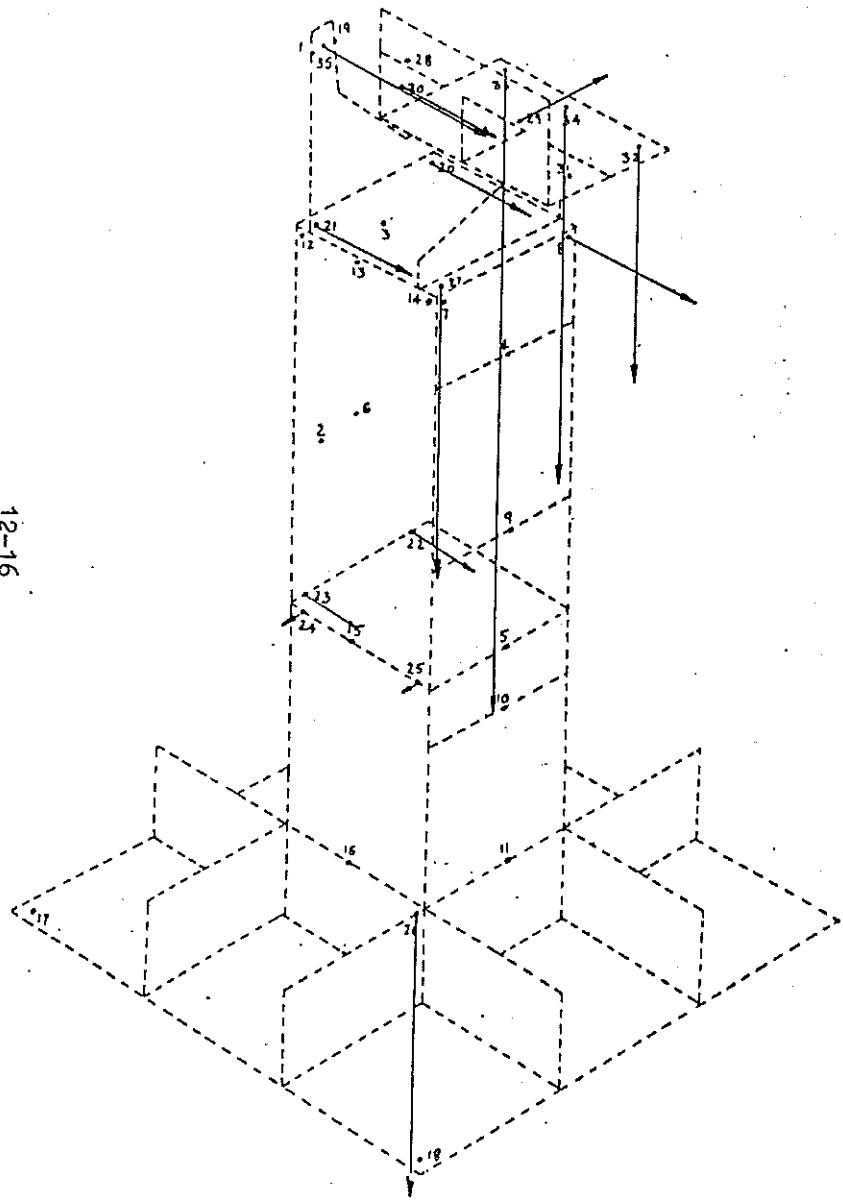
BUILD D

Description	Test Results (Hz)	NASTRAN Frequency (Hz)	% Error
1st Bending in Y direction	34.64	36.09	4.2
1st Bending in X direction	33.00	38.97	18.1
Torsion of top mass about Y	79.29	82.75	4.3
Torsion around Z	102.45	99.86	-2.57
Base plate panel modes		(148.41 (149.77 (152.16 (153.45	
Vertical Bounce	148.98	165.15	10.9
2nd Bending - X direction + torsion	192.43	171.47	-10.9
Panel modes of struct.	(222 (248		
Local mode of mass		234.03	
Panel mode of mass supports		250.94	
2nd Bending Y + torsion	264.8	271.51	2.53

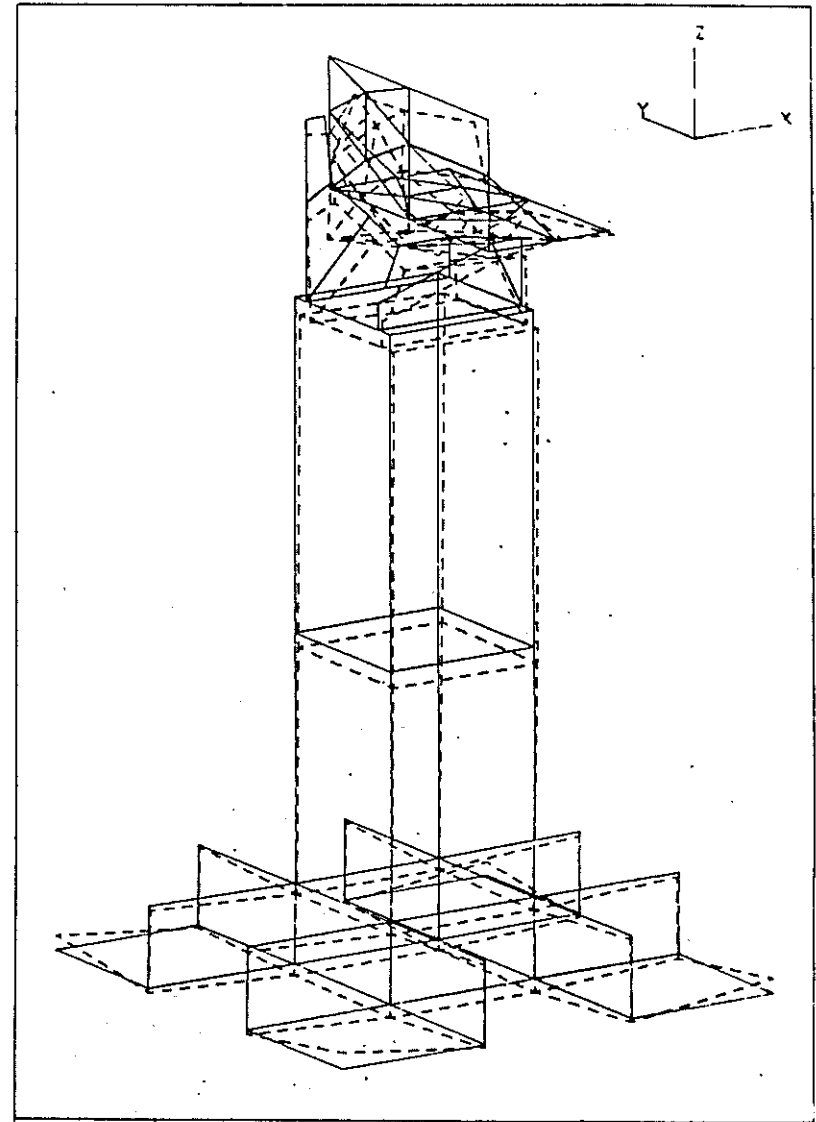
FIGURE 3

12-14

12-16



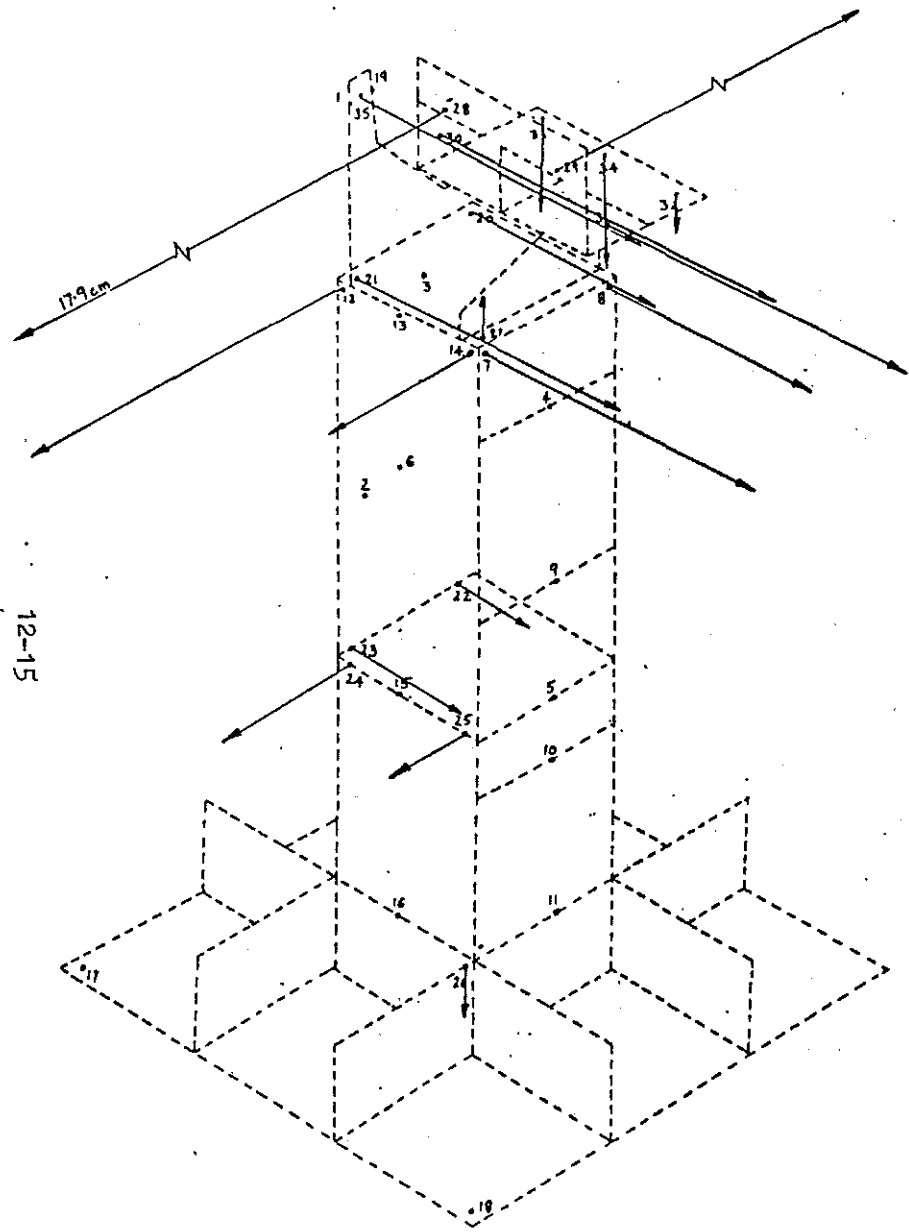
EXPERIMENTAL MODE SHAPE 148.98 Hz.



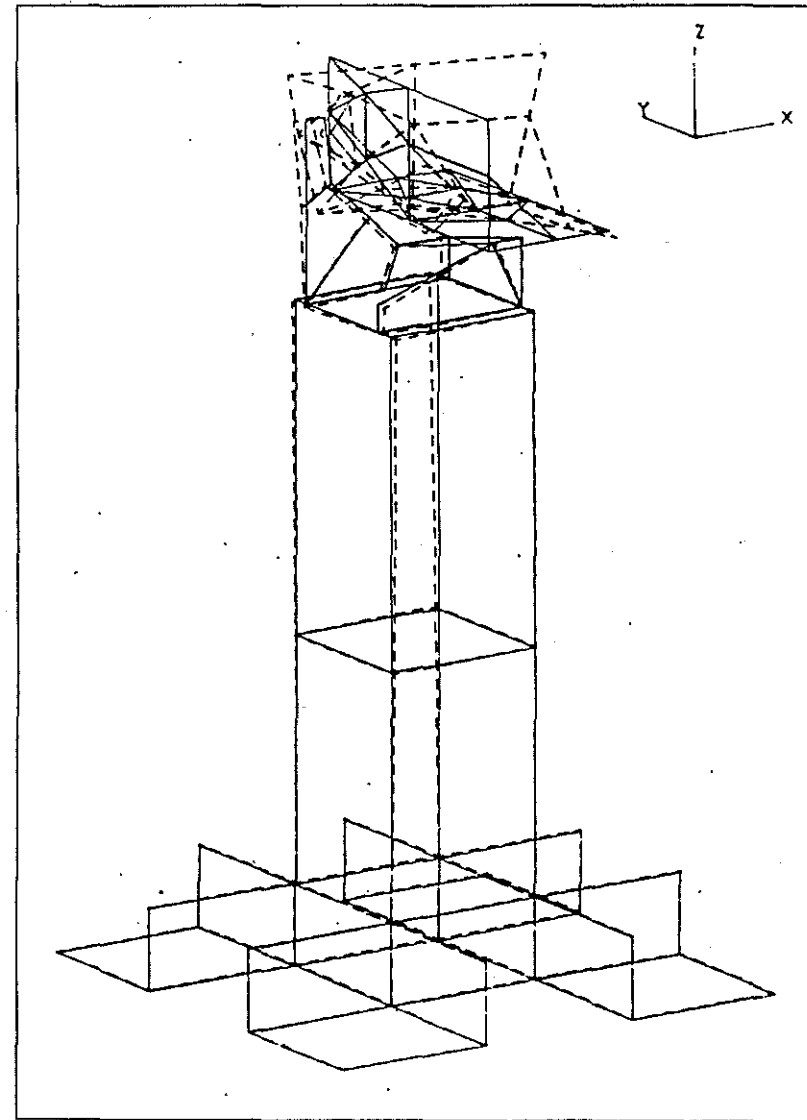
NASTRAN MODE SHAPE 165.15 Hz.

FIGURE 5

MODE SHAPE COMPARISON - BUILD D - TOP MASS TORSION



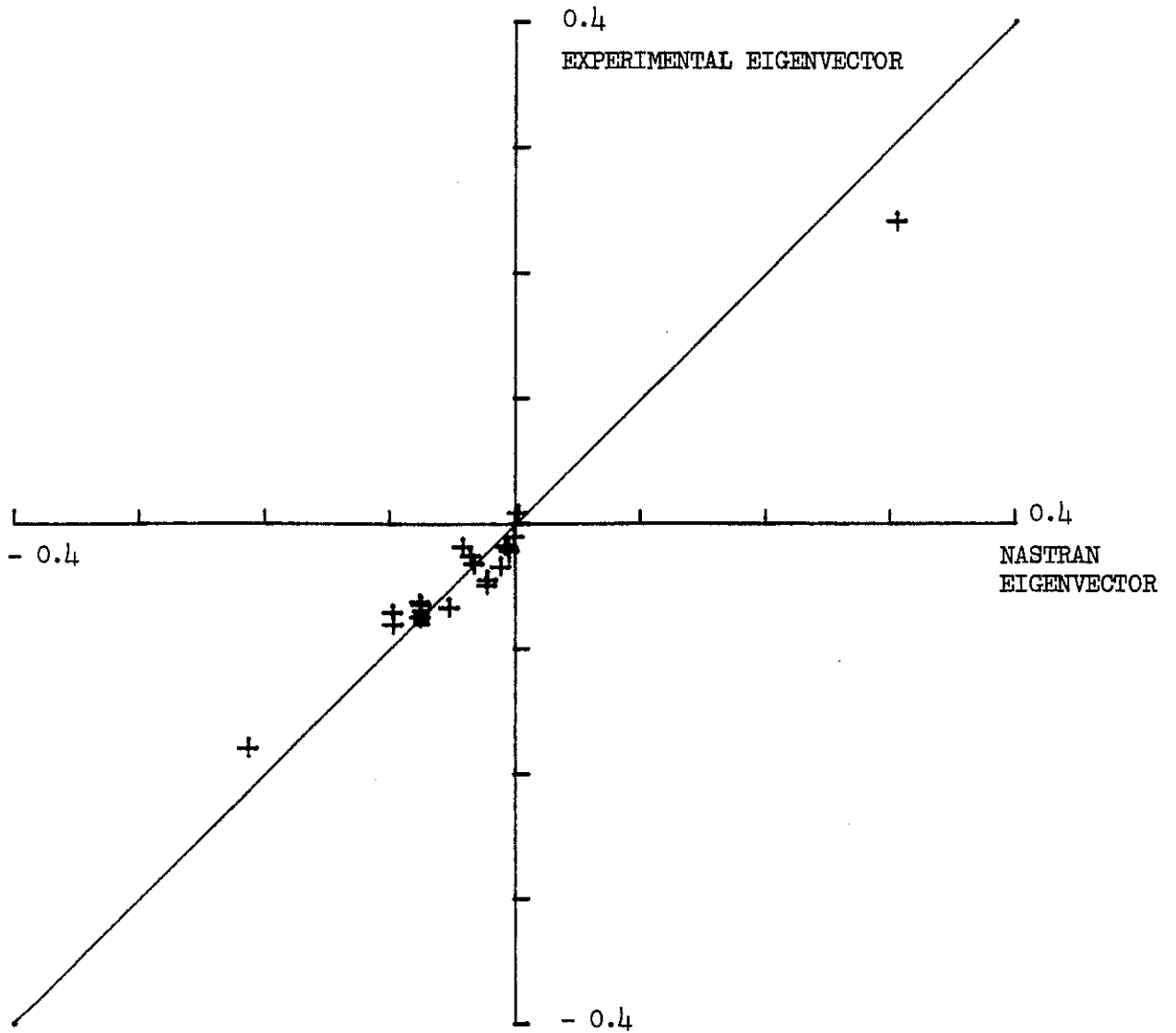
EXPERIMENTAL SHAPE 79.29 Hz.



NASTRAN MODE SHAPE 82.75 Hz.

FIGURE 4

COMPARISON OF DISPLACEMENTS

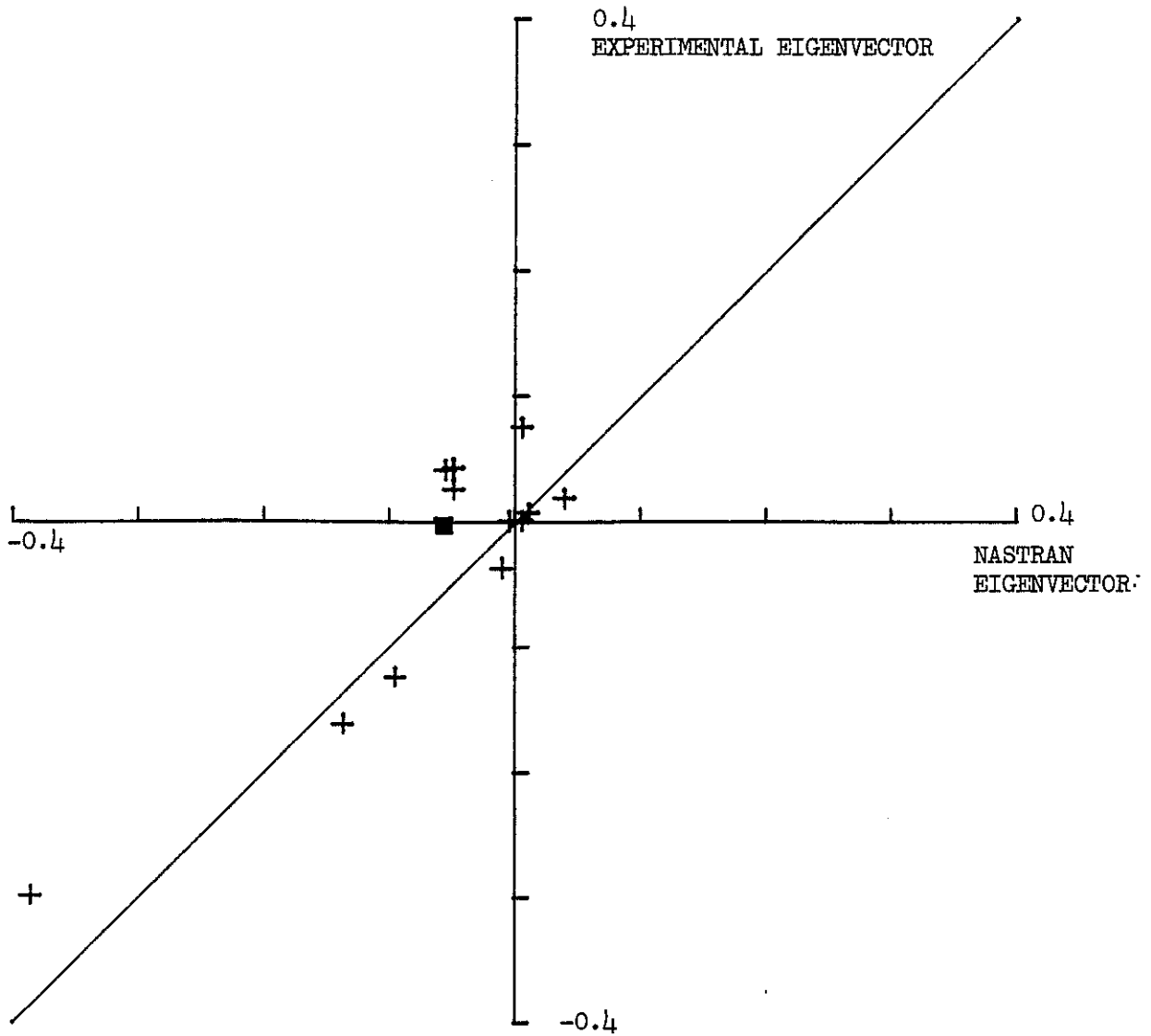


Vectors normalised to unit generalised mass

■ = point of excitation

BUILD D - TOP MASS TORSION (82.75 Hz.)

COMPARISON OF DISPLACEMENTS



Vectors normalised to unit generalised mass
= point of excitation

BUILD D - VERTICAL BOUNCE (165.15 Hz.)

REDUCTION TECHNIQUES

COMPARISON OF NATURAL FREQUENCIES

Mode Number (for GDR)	RUN 1 Generalised Dynamic Reduction	RUN 2 Guyan Reduction with 3 degrees of freedom on mass		RUN 3 Guyan Reduction with 6 degrees of freedom on mass	
	Frequency Hz	Frequency Hz	% Difference	Frequency Hz	% Difference
1	24.506	24.516	0.04	24.507	-
2	36.255	36.260	0.01	36.257	-
3	77.682	79.540	2.39	77.731	0.06
4	148.379*				
5	149.785*				
6	152.104*				
7	153.443*				
8	174.880	175.121	0.14	175.056	0.10
9	221.424	247.528	11.79	243.364	9.91
10	223.743	244.521	9.29	225.583	0.82
11	279.647*				
12	305.762	317.019		315.773	

* Panel or local mode

PAFEC ANALYSIS

RESULTS FOR BUILD CASE D

Mode No.	Description of Mode Shape	Measured Frequency (Hz)	Calculated Frequency (Hz)	Percentage Difference
1	Bending in X Direction	33.00	38.16	15.6
2	Bending in Y Direction	34.64	34.87	0.7
3	Mass Assemble Bending around Y	79.29	74.24	-6.3
4	Torsion around Z	102.5	107.41	4.8
5	Vertical Bounce	148.98	173.12	16.2
6	2nd Bending and Torsion in X	192.43	218.29	13.4
7	2nd Bending and Torsion in Y	264.8	284.39	7.4